High Free Cholesterol Bioavailability Drives the Tissue Pathologies in Scarb1−/− Mice

Jing Liu[1,2], **Baiba K. Gillard**[2,3,*], **Dedipya Yelamanchili**[2], **Antonio M. Gotto Jr.**[2,3], **Corina Rosales**[2,3], **Henry J. Pownall**[2,3,*]

[1]Department of Cardiovascular Medicine, Xiangya Hospital, Central South University, Changsha 410008, China,

[2]Center for Bioenergetics, Houston Methodist Research Institute, 6670 Bertner Avenue, Houston TX 77030, USA;

[3]Department of Medicine, Weill Cornell Medicine, 1300 York Ave, New York, NY, 10065, USA.

Abstract

Objective: Overall and atherosclerosis-associated mortality is elevated in humans with very high HDL-cholesterol concentrations. Mice with a deficiency of the HDL receptor, scavenger receptor, Class B, Type 1, (Scarb1) are a robust model of this phenotype and exhibit several additional pathologies. We hypothesized that the previously reported high plasma concentration of FC-rich HDL in Scarb1−/− mice produces a state of high HDL-FC bioavailability that increases whole-body FC and dysfunction in multiple tissue sites.

Approach and Results: The higher mol% FC in Scarb1−/− vs. WT HDL (41.1 vs. 16.0 mol%) affords greater FC bioavailability for transfer to multiple sites. Plasma clearance of autologous HDL-FC mass was faster in WT vs. Scarb1−/− mice. FC influx from Scarb1−/− HDL to LDL and J774 macrophages was greater (~4 times) than from WT HDL, whereas FC efflux capacity was similar. The higher mol% FC of ovaries, erythrocytes, heart, and macrophages of Scarb1−/− vs. WT mice are associated with previously reported female infertility, impaired cell maturation, cardiac dysfunction, and atherosclerosis. The FC contents of other tissues were similar in the two genotypes, and these tissues were not associated with any overt pathology. In addition to the differences between WT vs Scarb1−/− mice, there were many sex-dependent differences in tissue lipid composition and plasma FC clearance rates.

Conclusions: Higher HDL-FC bioavailability among Scarb1−/− vs. WT mice drives increased FC content of multiple cell sites and is a potential biomarker that is mechanistically linked to multiple pathologies.

Graphical Abstract

Corresponding Author: Henry J. Pownall, PhD, HJPownall@houstonmethodist.org, Houston Methodist Research Institute, 6670 Bertner Avenue, Room R11-217, Houston TX 77030, Telephone: (713) 441-7048.
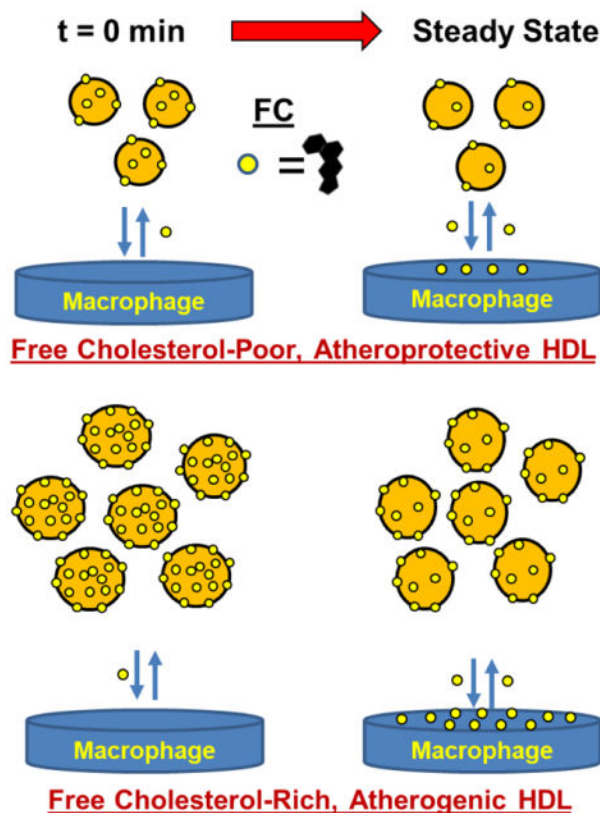*Shared Senior Authorship

c)*Disclosures:* Nothing to disclose.

Supplemental Materials
Online Figures I – V.
Online Tables I – VI.Expanded Materials and Methods

t = 0 min → Steady State

FC

○ = 🐾

Free Cholesterol-Poor, Atheroprotective HDL

Free Cholesterol-Rich, Atherogenic HDL

Keywords

Cholesterol; high density lipoproteins; hyperalphalipoproteinemia; scavenger receptor class B type 1; atherosclerosis

Subject Terms

Atherosclerosis; vascular disease; heart failure; cardiotoxicity; metabolic syndrome

Cholesterol has been implicated in the pathophysiology of atherosclerotic cardiovascular disease (ASCVD) for more than a century, beginning with the work of Anitschkow.[1] Early studies revealing an inverse relationship between plasma HDL-cholesterol (C) levels and ASCVD[2, 3] led to trials of HDL-raising interventions, which ultimately failed to reduce ASCVD.[4–7] More recently, several studies found higher ASCVD- and all-cause mortality risk among patients in both the lowest and highest quintiles for HDL-C concentration.[8–12] The cause of increased mortality in the highest HDL-C quintile is unknown but may be related to the reported differences in free cholesterol (FC) efflux.[13] According to a widely-cited model,[14–16] the macrophage FC burden associated with ASCVD is relieved by reverse cholesterol transport (RCT)—FC transfer from macrophages to HDL and plasma-mediated transport to liver and intestine for disposal.

Although subsequent studies showed that macrophage-FC efflux to HDL is a better inverse predictor of ASCVD than HDL-C concentration,[13, 17–19] not all subsequent studies[20–23] concurred. One of the causes of these disparate findings could be differences in HDL-FC bioavailability, which contributes to the reverse process, FC influx. FC flux between cells and HDL is bidirectional,[24–27] so that high plasma HDL-FC bioavailability could support FC transfer from HDL to arterial-wall macrophages in a way that counteracts and suppresses the putative salutary effects of macrophage FC efflux (Reviewed).[28] Because HDL-FC transfer occurs with $t_{1/2}$ ~5 min vs. 45 min for LDL,[29] HDL is, likely, the main source of plasma FC bioavailability, especially under conditions of high plasma concentration of HDL with high fractional FC content.[30, 31] Notably, FC flux between cells and HDL reverses from efflux to influx as HDL concentration, which is proportional to HDL-particle (P) concentration, increases, and its FC content rises above ~15 mol%;[32] with mol% FC defined as

$$\text{mol\% FC} = \text{mol}_{FC}/(\text{mol}_{FC} + \text{mol}_{PL}) \times 100\% \qquad \text{(Equation 1)}$$

where mol_{FC} and mol_{PL} are respectively the number of moles of FC and phospholipid (PL). These and other in vitro observations[24–26, 33, 34] provoked our formulation[28] of an HDL-FC bioavailability index (BI) as

$$\text{HDL-FCBI} = \text{HDL-P} \times \text{mol\% HDL-FC}/100 \qquad \text{(Equation 2)}$$

where HDL-P is the HDL particle number.

Moreover, HDL-FC is rapidly cleared by the liver in mice ($t_{1/2}$ ~ 5 min)[35, 36] and humans ($t_{1/2}$ ~ 10 min).[37] The HDL-receptor, scavenger receptor class B Type 1 (SR-B1), encoded by the *Scarb1* gene in mice, mediates cellular FC and CE uptake.[38] Scarb1^{−/−} mice, which exhibit impaired hepatic HDL-C uptake, have a plasma HDL-C concentration that is more than two-times higher than that of wild-type (WT), and an HDL-FC content (FC/particle) that is three times higher. Thus, according to Equation 1, Scarb1^{−/−} mice are a robust model of high HDL-FC bioavailability.[30, 31, 39, 40]

Elevated plasma HDL-FC among Scarb1^{−/−} vs. WT mice is associated with pathologies in heart,[41] the arterial wall (atherosclerosis),[30, 42] erythrocytes,[43, 44] adrenals,[45] thymocytes,[46] and ovaries.[47–49] We tested the hypothesis that these pathologies are due to the greater accretion of FC from HDL from Scarb1^{−/−} mice, which has a higher FC bioavailability compared to WT mice. To test this, we compared the in vitro transfer of Scarb1^{−/−} vs. WT mouse-HDL-FC to LDL and macrophages, in vivo HDL-FC clearance kinetics, and FC accretion by lipoproteins and tissue among Scarb1^{−/−} vs. WT mice of the same sex, and between male vs. female mice of the same genotype.

Materials and Methods

Disclosure:

The data that support the findings of this study are available from the corresponding author upon reasonable request.

Lipoprotein Isolation:

Lipoproteins were isolated from pooled mouse plasma (5–10/genotype) by sequential flotation.[50, 51] Purity was verified by size exclusion chromatography (SEC)[52] and compositional analyses. HDL from individual mice was isolated by heparin-manganese precipitation of plasma APOB lipoproteins.[29, 53] Plasma and tissue lipids were determined using enzyme-based assays for FC, total cholesterol (TC), PL, and triglyceride (TG) (Fujifilm Wako Diagnostics Inc.). Cholesterol ester (CE) concentrations were calculated as (mg TC – mg FC) $\times$ 1.6. . Protein was determined by the DC Protein Assay (Bio-Rad, Inc.).

In Vitro HDL-FC Transfer Kinetics:

HDL was radiolabeled with [^{3}H]FC as described previously.[36] Specific activities (dpm/nmoles FC) were calculated on the basis of HDL-FC concentration and β-counting of aliquots. To assay rates of transfer of HDL-FC to LDL, HDL-[^{3}H]FC (10 μg protein/mL) was incubated with human LDL (1.0 mg/mL) at 37 °C. Aliquots were removed over time and LDL precipitated.[29, 53] Supernatants were β-counted and counts vs. time data and fitted to a three-parameter exponential decay equation from which kinetic constants were extracted.

Equilibrium Distribution of [^{3}H]FC between LDL and HDL:

HDL-[^{3}H]FC transfers to LDL with $t_{1/2}$ ~5 min.[29] We incubat human LDL and various concentrations of HDL-[^{3}H]FC for ~18 h at 37 °C after which HDL was separated from LDL by size exclusion chromatography. Fractions were collected and β-counted, and [^{3}H]FC transfer from HDL to LDL was based on LDL-associated radioactivity. HDL-[^{3}H]FC to LDL transfer was based on the slopes of LDL-associated FC mass vs. the various HDL-protein or HDL-FC concentrations.

FC Flux between HDL and Macrophages:

FC flux between HDL and J774 macrophages (J774A.1, ATCC® TIB67™) were measured essentially as described.[34, 52, 54–56] To quantify FC influx, [^{3}H]FC-labeled HDL was incubated with macrophages and cell-associated [^{3}H]FC was measured as a function of HDL concentration and time.[52, 56] Influx dose-response was assayed at 2 h and analyzed using a two-parameter hyperbolic function. For time course experiments, [^{3}H]FC-labeled HDL was incubated with macrophages for various times. Uptake kinetics were fitted to a rising exponential function. FC efflux to HDL was measured by incubating HDL with [^{3}H]FC-labeled macrophages as described.[34] Respective time- and concentration-dependence of efflux were fitted to exponential and hyperbolic equations as described for influx. Initial rates of influx and efflux were determined from the fitted time-course equations.

Mouse Management and Tissue Analysis:

Mice (The Jackson Laboratory), maintained on normal laboratory diet, were studied at 12–25 weeks of age except where stated otherwise. Retro-orbital injections of HDL-[^{3}H]FC were conducted after isoflurane inhalation to achieve an anesthetic effect. Mice were euthanized and their blood collected by heart puncture into EDTA; tissues

were harvested.[57–59] Tissues were weighed, homogenized, and extracted. Tissue-protein was solubilized with 0.4 M NaOH + 1% sodium dodecyl sulfate. Extracted lipids were dissolved in 1% Triton in chloroform, which was evaporated, and solubilized in water.

In Vivo HDL-FC Metabolism:

Mice were retro-orbitally injected with HDL-[^{3}H]FC, and euthanized at various times post-injection. Blood was collected and centrifuged to sediment cells, and the supernatant β-counted. Erythrocytes were washed, lipid-extracted, and protein determined as above. Kinetic data were fitted to a two-parameter exponential function of percent injected dose vs. time; initial rates were calculated as the percent change/min between t = 0 and 2 min.

Statistical Analysis:

Data are presented as mean ± standard deviation (SD) or standard error of the mean (SEM). Group means were compared by Student's t-test. Regression analyses and comparison of linear regression slopes and intercepts were were performed in SigmaPlot 12.0 or Prism 8.0. Differences in compositions were identified by pairwise comparisons when the analysis of variance indicated significance. Data were tested for normality and Equal Variance, and if passed, pairwise comparisons were done using the All Pairwise Multiple Comparison Procedures or Student's t-test. If the data failed normality or equal variance tests, the Kruskal-Wallis one-way analysis of variance on ranks or a rank-sum test were used for pairwise comparisons and calculation of p-values.

Results

Plasma and HDL-FC Bioavailability:

FC partitions almost exclusively into its essential "solvent," PL, within the cellular plasma membrane and on the surface of HDL. The relative amount of FC compared to PL is one determinant of HDL-FC bioavailability, expressed as mol% FC, (Equation 1). According to our hypothesis and previous report,[32] the higher mol% FC in the HDL of Scarb1$^{-/-}$ vs. WT mice is part of our metric for FC bioavailability; the other is the total number of HDL particles, HDL-P (Equation 2).

Comparison of the lipid concentrations of plasma from WT and Scarb1$^{-/-}$ mice (Figure 1) confirmed previous reports[30, 31] that TC, FC and CE are higher in Scarb1$^{-/-}$ mice for males and females; plasma PL is higher in female Scarb1$^{-/-}$ mice. CE and PL are elevated in male vs. female WT mice. Accordingly, the mol% plasma FC is also higher in the Scarb1$^{-/-}$ vs. WT mice (Figure 1 B), respectively +69% for female mice and +136% for male mice. The FC/TC ratios were also higher in female and male Scarb1$^{-/-}$ mice, +178% and +223% respectively (Figure 1 C). The HDL lipid profiles simulate those of whole plasma (Figure 1 D–F). Analysis of the data of Figure 1 D showed that the sums of the plasma concentrations of HDL-PL, FC, and CE for Scarb1$^{-/-}$ female and male mice vs. those of WT mice are 95 and 55% higher so that the HDL concentration among Scarb1$^{-/-}$ mice is greater than that of WT. HDL compositional analysis for both genotypes indicated that HDL-TG <0.5% of the total HDL mass and HDL-protein is 41% and 37% of the total for WT and Scarb1$^{-/-}$ mouse HDL respectively (Supplementary Figure I and Supplementary Table I). Thus, plasma HDL

concentration is higher among Scarb1$^{-/-}$ vs. WT mice. Importantly, compared to the other lipids, there was a larger difference in the plasma FC concentrations of the Scarb1$^{-/-}$ vs. WT mice—FC is 8.2- and 6.8- fold higher in the Scarb1$^{-/-}$ female and male vs. their WT counterparts, respectively. Others have reported similar but less profound elevations,[30, 31] which are smaller among mice in which APOE levels are suppressed.[39] These data support our hypothesis that the higher HDL-FC content as mol% FC drives the higher HDL-FC bioavailability among Scrab1$^{-/-}$ vs. WT mice.

Scarb1 Deletion Alters Lipoprotein Compositions:

Compared to HDL from WT mice, HDL from Scarb1$^{-/-}$ mice is PL-poor and both CE-, and especially FC-, rich (Supplementary Table I). Again, the mol% FC in Scarb1$^{-/-}$ HDL is higher than that of WT, 41.1 ± 2.4 vs. 16.0 ± 4.3%. Scarb1-deletion also increased the FC content and the mol% FC in the very low- and low-density fraction (VLDL + LDL; Supplementary Table I). As previously reported by others,[30, 31, 39, 42] the HDL-FC/TC ratio is also higher among Scarb1$^{-/-}$ vs. WT mice. Thus, Scarb1-deletion increases the mol% FC in HDL and LDL and the FC/TC ratio.

In Vitro HDL-FC to LDL Transfer Kinetics:

According to our model (Supplementary Figure II), a high HDL-FC content supports enhanced FC transfer to other lipoproteins and tissues. Scarb1$^{-/-}$ mice have three times more HDL-FC content, i.e. more FC per particle (Figure 1, Supplementary Figure I, and Supplementary Table I), and when receiving a high fat-high cholesterol diet, more HDL particles, a condition that induces atherosclerosis.[31] As illustrated by our model, mass action drives more FC transfer from the FC-rich HDL of Scarb1$^{-/-}$ mice to all lipid surfaces, other lipoproteins and cell membranes, than from the relatively FC-poor HDL of WT mice. The model also predicts that at equilibrium the higher particle number and mol% FC in Scarb1$^{-/-}$ vs. WT HDL drives the increased transfer of HDL-FC to other lipid surfaces in contact with plasma.

We conducted two in vitro tests comparing the FC bioavailability of WT and Scarb1$^{-/-}$ mouse HDL and human HDL. First, we incubated LDL (800 μg/mL protein) with various concentrations of HDL-[^{3}H]FC for 18 h, which allowed [^{3}H]FC to distribute between HDL and LDL until reaching equilibrium, and then determined the LDL-associated FC by SEC (Supplementary Figure III). The slopes of LDL-associated FC vs. HDL protein indicated that two-times more FC transferred from Scarb1$^{-/-}$ HDL to LDL than from WT and human HDL to LDL (Figure 2 A). However, when comparing HDL-FC transfer to LDL on the basis of the initial HDL-FC concentrations, the amount transferred from all three HDL species to LDL linearly correlated with the amount of donor FC (Figure 2 B). Notably, for a given HDL species, transfer increased with initial HDL-FC concentration and was greatest for Scarb1$^{-/-}$ HDL (⬤), which has the highest mol% FC.

In the second experiment, we incubated [^{3}H]FC-labeled HDL with LDL, and measured the rates of HDL-associated [^{3}H]FC transfer as described.[29, 35, 52, 53] Rate constants for transfer from the three HDL species were slightly different with [^{3}H]FC transfer from Scarb1$^{-/-}$ HDL being 30% slower than transfer from WT HDL (Figure 2 C–E). However,

the amount transferred at equilibrium ($\Delta_{transfer}$) was ~3.0–3.5 times greater (589, 167, and 197 pmol/mL respectively) for Scarb1$^{-/-}$ vs. WT mouse and human HDL (Figure 2 C–F). These observations suggest that the higher HDL-FC content of Scarb1$^{-/-}$ vs. WT and human HDL[31] drives more FC mass transfer to other lipid surfaces, in this case, LDL. Because the rate-limiting step for HDL-FC transfer to all tissue and lipoprotein sites is the initial desorption step,[29, 60] HDL-FC transfer to LDL is a potential metric for HDL-FC bioavailability and transfer to all tissues and lipoproteins.

Kinetics of FC Flux between HDL and J774 Macrophages:

Whereas feeding a high-fat, high-cholesterol diet to Scarb1$^{-/-}$ mice induces ASCVD, changes in plasma concentrations of atherogenic APOB-containing lipoproteins are minimal, while plasma HDL concentrations increase two-fold.[30] Thus, among Scarb1$^{-/-}$ mice, an increase of HDL or of one of its components is mechanistically linked to atherosclerosis. Because macrophages and their conversion to foam cells within the arterial wall are hallmarks of ASCVD, we determined the kinetics of HDL-FC flux between WT and Scarb1$^{-/-}$ mouse HDL and, for comparison, human HDL, and J774 macrophages in terms of influx from HDL to cells and efflux from cells to HDL (Figure 2, Supplementary Table II). Both the initial rate constant k_i for FC influx[25, 26] and the influx$_{max}$ from HDL to macrophages were 4.1 fold higher in Scarb1$^{-/-}$ than WT mice. (Figure 2 G; Supplementary Table II). HDL-FC influx was HDL concentration-dependent and differed among the three kinds of HDL. The maximum influx from Scarb1$^{-/-}$ HDL was 3.1 times that of WT, while the HDL protein concentration that produced 50% of maximum uptake was lower (−25%) than that of WT (Figure 2 H, Supplementary Table II). Similarly designed FC efflux studies showed that FC efflux from macrophages to WT and Scarb1$^{-/-}$ mouse and human HDL was similar with respect to time- and dose- dependence (Figure 2 I, J; Supplementary Table II). Thus, as with HDL-FC transfer to LDL, more FC is transferred to macrophages from Scarb1$^{-/-}$ HDL than from WT HDL, while mouse and human HDLs are comparable acceptors of macrophage FC, resulting in greater FC accretion by cells incubated with Scarb1$^{-/-}$ vs. WT HDL.

Elevated FC and Mol% FC in Erythrocytes, Heart, Lung, and Female Liver of Scarb1$^{-/-}$ vs. WT Mice.

HDL-FC is rapidly extracted by the liver and over longer times, HDL-FC transfers to all major tissues.[35–37] Thus, we tested whether tissue-FC content among Scarb1$^{-/-}$ mice was higher than that among WT mice due to higher mol% HDL-FC in Scarb1$^{-/-}$ mice. Our findings were sex- and tissue site-dependent (Figure 3, Supplementary Table III). Both FC content and mol% FC were significantly higher in erythrocytes, heart, lung and female liver of Scarb1$^{-/-}$ vs. WT mice (Figure 3 A, B, D, E, G, H, J, and K). The mol% FC can be increased by reducing the PL content or by increasing FC content (Equation 1). In support of our hypothesis, the mol% FC in Scarb1$^{-/-}$ erythrocytes was higher than in WT erythrocytes (Figure 3 A, B,) and increased by Scarb1 deletion more than any other site studied (+23%) except for ovaries (see below); this effect was due solely to higher FC content and not lower PL content (Equation 1). The effect on heart and lung FC was smaller, +21.4% and +15.7% respectively (Figure 3 D, E, and G, H). In liver, the mol% FC was higher in Scarb1$^{-/-}$ than in WT female mice but not among male mice (Figure 3 K). The erythrocyte,

heart- and liver-FC/TC ratios were similar for the two genotypes but lower for lung among Scarb1$^{-/-}$ vs. WT mice (Figure 3 C, F, I, L). CE was more than 4-fold elevated in Scarb1$^{-/-}$ lung (Figure 3G) and in male Scarb1$^{-/-}$ erythrocytes (Figure 3A). Scarb1-deficiency did not affect heart and lung triglyceride (TG) content, whereas hepatic TG was reduced, and erythrocyte TG was increased by Scarb1-deletion in male but not female mice (Figure 3 A, D, G and J).

Fat Depots:

The effects of Scarb1-deletion on the lipid compositions of fat were sex- and depot-specific (Figure 4). As expected, TG was the major lipid within all three fat depots tested, thus the TG data are presented at 1/20 their determined values to allow comparison with other lipids on the same scale. While we found no sex- or genotype-specific differences in the TG content of abdominal fat, we did find some significant differences in the PL, TC, FC, and CE content of abdominal fat based on sex and/or phenotype (Figure 4 A). The FC and mol% FC within abdominal fat of Scarb1$^{-/-}$ vs. WT mice were higher among male but were not different for the two female genotypes (Figure 4 A, B). Abdominal fat FC/TC ratios for Scarb1$^{-/-}$ and WT mice of the same sex did not differ, but within genotype, the FC/TC ratios of male mice were lower than those of female mice. Within ovary fat, the lipid compositions and mol% FC of Scarb1$^{-/-}$ and WT mice showed no remarkable differences although the FC/TC ratio was higher (+100%) for WT mice (Figure 4 D, E, F). In contrast, the mol% FC in testes fat was higher in Scarb1$^{-/-}$ mice than in WT mice whereas the FC/TC ratio was lower (Figure 4 H, I). These data are consistent with FC accretion in fat depots of male but not female Scarb1$^{-/-}$ mice.

Scarb1 Deletion Alters Ovary and Adrenal but not Testis FC Content.

CE is reduced while mol% FC is increased in Scarb1$^{-/-}$ ovaries while the cholesterol composition in Scarb1$^{-/-}$ testes does not differ from WT. However, these data may not fully reflect the impact of FC bioavailability on Leydig cells, the testosterone-producing cells, because they are only a small fraction of testes mass. Ovary-PL and CE contents were lower in Scarb1$^{-/-}$ than in WT mice, 25 vs. 90 and 76 vs.179 µg/mg protein, respectively (Figure 5 A; Supplementary Table III). Scarb1$^{-/-}$ ovaries exhibited a higher mol% FC than did WT ovaries (Figure 5 B). High mol% FC results from either high FC content or low PL content (Equation 1), and in this case was due largely to the 70% lower ovary-PL content in Scarb1$^{-/-}$ mice. Ovary-FC contents of both mouse genotypes were similar despite the large decrease in total cholesterol in Scarb1$^{-/-}$ mice (Figure 5 A). These data are supported by the FC/TC ratios in Scarb1$^{-/-}$ (0.34) and WT (0.20) mice, reflecting in part, the intracellular conversion of FC to CE. Notably, ovary CE content is more than an order of magnitude greater than in all other tissues tested other than adrenal tissue (see below and Supplementary Table III), with the next highest CE content in brain at ∼ 1/10 that of ovaries. The ovary CE content is reduced by half in Scarb1$^{-/-}$ female mice. Ovary-TG content did not differ among the two genotypes. In contrast, the lipid compositions of testes from Scarb1$^{-/-}$ and WT mice were similar for PL, TC, FC, and CE, while TG was reduced, 49 ± 14 vs 84 ± 34 µg/mg protein (Figure 5 D–F). Within the adrenals, there were differences in lipid composition according to sex and genotype. Adrenal TC values were 3 and 6 fold lower in Scarb1$^{-/-}$ female and male mice compared to WT mice, respectively, similar to

values previously reported for Scarb1$^{-/-}$ and WT mice.[40] Scarb1-deficiency increased the adrenal-PL content, whereas male mice had lower adrenal-PL than female mice (Figure 5 G). FC was also increased in Scarb1$^{-/-}$ male vs WT mice, and FC was higher in females vs. males of both genotypes. The net effect of similar changes in adrenal-FC and PL with respect to genotype was non-significant differences in adrenal mol% FC (Figure 5 H). However, mol% FC was lower in males than females of both genotypes. In contrast, Scarb1 deficiency greatly reduced adrenal-CE (>85%) and was also lower in male vs. female mice. The FC/TC ratios were also different, ~5 and ~25-times higher for male and female Scarb1$^{-/-}$ vs. WT mice (Figure 5 I).

Lipid Compositions of Brain, Kidney, and Spleen:

Brain, kidney, and spleen were resistant to the high FC bioavailability associated with Scarb1-deletion (Supplementary Figure IV, Supplementary Table III). Although there were some significant differences in mol% FC and the FC/TC ratio of brain, kidney, and spleen of Scarb1$^{-/-}$ vs. WT mice, they were small compared to changes in other tissues and likely not physiologically meaningful. Of note, kidney mol% FC was lower in males than females for both Scarb1$^{-/-}$ and WT mice (Supplementary Figure IV E).

In vivo HDL-FC Metabolism:

Comparison of plasma HDL-[^{3}H]FC clearance kinetics revealed differences in both the rates and magnitude (Figure 6 A; Supplementary Table IV). Following injection with autologous HDL-[^{3}H]FC, initial and overall rates for [^{3}H]FC plasma clearance were ~60% and 20% faster for WT mice compared to Scarb1$^{-/-}$ mice and faster for female mice. In addition, the decays to asymptotes were greater for WT than for Scarb1$^{-/-}$ mice for both females and males. The decay asymptotes, which represent equilibrium FC distribution, were higher for Scarb1$^{-/-}$ mice, i.e. 38% vs. 8% with clearance of 62% and 92% into the rapidly exchanging tissue FC pool. Using the averages for male and female mice, plasma FC concentrations for WT and Scarb1$^{-/-}$ mice were 0.18 and 1.3 mg/mL (Figure 1 A). Thus, the total exchangeable FC pool sizes are 0.18/0.08 and 1.3/0.38 or 2.3 and 3.4 mg. In contrast, the respective rapidly exchangeable tissue-pool sizes are 2.3 mg – 0.18 mg = ~2.1 mg and 3.4 mg – 1.3 mg = 2.1 mg.

Despite the faster rate constant for the clearance of HDL-FC for WT vs. Scarb1$^{-/-}$ mice, the amount of HDL-FC cleared per unit time is greater for Scarb1$^{-/-}$ mouse HDL-FC. Whereas the within-genotype HDL-FC pool sizes are similar, the Scarb1$^{-/-}$ HDL-FC pool size (plasma HDL-FC concentration, Figure 1 D) is larger than that of WT. According to the initial percent change (Figure 6, Supplementary Table IV) and the HDL-FC concentrations (Figure 1 D), within sex, 3-times more HDL-FC mass is cleared by Scarb1$^{-/-}$ vs. WT mice (Supplementary Table IV, next to last column). Thus, the large HDL-FC pool size among Scarb1$^{-/-}$ vs. WT mice leads to a greater mass of HDL-FC cleared per unit time.

In the same experiment we measured [^{3}H]FC accretion by erythrocytes. These data (Figure 6 B) showed a rapid increase within the first 2 min for males and females of both mouse genotypes after which accumulation of [^{3}H]FC in the WT mice plateaued. The beginning of the plateau corresponded to the time at which plasma-[^{3}H]FC among WT mice was near nil

(arrows in Figure 6 A, B). In contrast, erythrocyte- [^{3}H]FC continued to increase up to the final time point (90 min) in the Scarb1$^{-/-}$ mice, an effect that was more profound in female mice.

Discussion

The Scarb1$^{-/-}$ mouse is a robust model of dysfunctional HDL; HDL from Scrarb1$^{-/-}$ vs. WT mice is distinguished by a high plasma concentration of HDL that is FC- and CE-rich.[30, 31] These observations provoked our tests of the hypothesis that tissues and/or cells in contact with a high plasma concentration of FC-rich HDL are FC-rich. Using mol% FC, which compares the relative amount of FC vs. PL, the FC solvent, we confirmed the reports of others, finding that compared to WT, Scarb1$^{-/-}$ HDL is FC-rich, i.e., has a higher mol% FC. We then tested whether surfaces in contact with plasma of Scarb1$^{-/-}$ vs. WT mice are more FC-rich. Comparisons revealed our new findings as follows: The magnitude of FC transfer from Scarb1$^{-/-}$ HDL to LDL is greater than that from WT HDL; APOB-containing lipoproteins from Scarb1$^{-/-}$ vs. WT mice are FC-enriched due likely to the greater transfer from FC-rich HDL. While macrophage efflux to HDL of Scarb1$^{-/-}$ vs. WT HDL was not different, FC influx from Scarb1$^{-/-}$ vs. WT HDL to macrophages was three-fold greater, a net effect that increases macrophage-FC burden. We were first to compare the FC, CE, PL, and TG contents of all major tissues and identify differences. We determined that FC accretion by some tissues is higher among Scarb1$^{-/-}$ vs. WT mice whereas in other tissue FC homeostasis is maintained despite Scarb1 deletion. We determined that the rate of autologous plasma HDL-FC clearance is slower among Scarb1$^{-/-}$ vs. WT mice. Lastly, we determined that the tissue compositions and plasma FC clearance kinetics varied according to sex, particularly among Scarb1$^{-/-}$ mice. These findings are relevant to pathologies specific to Scarb1$^{-/-}$ mice and to the evolving model of the role of HDL-FC in human RCT.

Cell membranes and plasma lipoproteins contain numerous lipids that are indispensable to metabolism. FC is physiologically distinctive because it is a precursor to bile salts and other steroidogenic molecules that are metabolic regulators.[61–63] FC is physico-chemically distinctive because it transfers rapidly among lipid surfaces[29] and eventually diffuses to all tissues independent of a carrier.[36] Although the reported halftime for FC transfer from HDL to LDL, ~5 min,[29] was confirmed by our studies, there were differences. First, FC transfer from the larger Scarb1$^{-/-}$ vs. WT HDL was slower, a finding consistent with Kelvin's law predicting an inverse relationship between transfer rates and particle radius[29, 60, 64] Second, and relevant to Scarb1$^{-/-}$ pathophysiology, at equilibrium Scarb1$^{-/-}$ HDL delivered more FC to LDL than did WT HDL. Thus, the higher mol% plasma FC for Scarb1$^{-/-}$ produced a state of increased plasma FC bioavailability. Given that the increases in mol% plasma and HDL-FC in Scarb1$^{-/-}$ mice were similar and that HDL contains more >90% of plasma FC,[31] the underlying cause of high plasma mol% FC is due to the higher mol% HDL-FC ,[30, 31, 42] which transfers to LDL increasing the mol% LDL-FC. This is consistent with the observed elevated plasma LDL-FC in LDL receptor-deficient mice with attenuated Scarb1 expression.[65] Whereas FC bioavailability expressed as mol% FC could be reduced by lower FC and/or higher PL, HDL-PL content is genotype-independent whereas HDL-FC content is higher in Scarb1$^{-/-}$ vs. WT mice. The ten-times faster rate of HDL- vs. LDL and VLDL

lipid desorption[29, 60] potentiates HDL-FC bioavailability, which is relevant to LDL-receptor mediated FC-disposal in humans[66] and trans-intestinal cholesterol excretion.[67]

Excess HDL-FC among Scarb1^{−/−} mice due to the loss of the terminal RCT step, hepatic FC uptake, has been implicated in many of the pathologies of this mouse model, including diet-induced atherosclerosis.[30, 39, 42] Our ex vivo studies of FC flux between J774 macrophages and HDL provides a mechanistic link between excess HDL-FC and atherosclerosis by revealing more FC influx from Scarb1^{−/−} HDL than from WT HDL without meaningful differences in efflux. Notably, cholesterol efflux to the APOB-depleted plasma of a patient with SCARB1-deficiency was not different from that of controls.[68]

Macrophage FC efflux to APOB-depleted plasma is an ASCVD proposed risk-metric for peripheral tissue-FC transfer to HDL, including arterial-wall macrophages to HDL transfer.[13] Despite the importance of HDL in this process, APOB-containing lipoproteins are also FC acceptors and although HDL is the initial acceptor of FC efflux, most FC transfers to LDL within 30 minutes.[69] In humans, the FC recycling between HDL and LDL and between HDL and tissue, which has been quantified,[36, 70] supports the hypothesis that FC readily transfers among multiple tissue-, cell-, and lipoprotein-surfaces. In vitro bidirectional FC flux between HDL and cells is well-documented.[24–27] Our data bring new in vitro, ex vivo, and in vivo insights into the role of FC bioavailability at the interface of tissues and lipoproteins by showing that the balance between influx and efflux is a function FC bioavailability in a mouse model of high HDL-FC bioavailability. Our data support the hypothesis that the reported ASCVD in these mice is due to an imbalance of FC flux between HDL and tissues with >4-times higher HDL-to-macrophage influx/efflux ratios for Scarb1^{−/−} HDL than for WT HDL.

Whereas the endogenous LCAT activity in Scarb1^{−/−} is ~90% lower than that of WT mice,[31] LCAT overexpression in Scarb1^{−/−} mice reduces the plasma HDL-FC/PL ratio and with it, FC bioavailability, which may suppress, as reported, diet-induced atherosclerosis.[71] The disturbances of FC homeostasis by Scarb1 ablation could be a direct consequence of the loss of SR-B1 or a secondary effect of reduced LCAT activity. Current evidence suggests roles for both. The absence of hepatic selective HDL-CE uptake in Scarb1^{−/−} mice[30] increases plasma HDL-CE. Given that SR-B1 also clears cellular HDL-FC, Scarb1 deletion could also increase plasma concentration of HDL-FC, which transfers to cells by spontaneous and SR-B1-mediated mechanisms.[38] Superposition of a 90% decrease in LCAT activity on lower hepatic FC uptake would increase the FC to TC ratio as reported.[71]

Initial and total kinetics of plasma HDL-[3H]FC clearance in WT mice were ~60% and ~20% faster than those in Scarb1^{−/−} mice, reflecting the absence of Scarb1, which clears many lipids including FC,[38] which is initially cleared by the liver.[35–37] Although the cholesterol content of a mouse is 2.2 mg/g or 66 mg/30 g mouse,[72] the amount in liver is, as expected, a fraction of this, 12 mg, and the amount in a rapidly exchangeable hepatic pool is smaller yet, by our calculations, ~2 mg/mouse. After an initial rapid uptake of ~60% of injected HDL-[3H]FC, hepatic [3H]FC content declines over longer times due to excretion and transfer to erythrocytes[43] and tissues.[36] Consistent with this, in our study, the rate and magnitude of [3H]FC appearance in erythrocytes was similar among all mice during

the first ~10 min, after which erythrocyte-[^{3}H]FC plateaued among WT mice but continued to increase in Scarb1$^{-/-}$ mouse erythrocytes. We attribute this difference to the persistence of 40% of injected HDL-[^{3}H]FC in plasma beyond 10 min in Scarb1$^{-/-}$ mice, which have a continuous pool of HDL-[^{3}H]FC that transfers FC to erythrocytes. This increased [^{3}H]FC accretion is consistent with higher erythrocyte-FC in Scarb1$^{-/-}$ than in WT mice.

Among WT female and male mice, the respective rate constants for HDL-FC clearance, which includes both Scarb1-dependent and independent mechanisms (spontaneous diffusion) are $k_1 = 1.27$ and 0.72 min^{-1}. Scarb1 deletion reduces the rate constants to 0.86 and 0.59 min^{-1}, respectively, i.e., 68 and 82% of WT k_1, indicating that Scarb1 accounts for less than half the clearance, and thus spontaneous diffusion is a major contributor to FC clearance. Whereas hepatic FC clearance occurs by these two mechanisms, most CE is cleared via Scarb1, which gradually reduces the size of HDL by a slower[73] "nibbling" mechanism,[74] which is independent of apolipoprotein or holoparticle uptake.

Whereas we hypothesized that the higher HDL-FC bioavailability in Scarb1$^{-/-}$ mice vs. WT mice would support increased tissue-FC accretion this is opposed by numerous mechanisms supporting cholesterol homeostasis. High HDL-FC bioavailability in Scarb1$^{-/-}$ vs. WT mice enhanced HDL-FC transfer to LDL and influx into macrophages. On this basis, we expected higher FC content in tissues of Scarb1$^{-/-}$ vs. WT mice. This was observed only for erythrocytes, heart, lung, liver (females only), adrenals (males only), abdominal fat (males only), and testes fat. No difference between the FC of WT and Scarb1$^{-/-}$ mice was observed in the other tissues assayed, although the mol% FC was elevated in Scarb1$^{-/-}$ vs. WT ovaries due to lower ovary-PL content. In particular, the FC content of brain, the organ with the highest FC content, was similar in Scarb1$^{-/-}$ and WT mice, as reported.[75] This may be due to the isolation of the brain from the rest of the body by the blood-brain barrier; most brain FC is synthesized in situ, not imported. Moreover, in the adult mouse, brain-FC is exported to plasma.[75] Although the tissue pathologies in Scarb1$^{-/-}$ were profound, they occurred under conditions of only modestly higher tissue FC content compared to WT mice, i.e. +15–22%, thus illustrating the importance of finely controlled FC homeostasis. By the same token, the higher macrophage uptake of FC from Scarb1$^{-/-}$ vs. WT HDL might be expected to be pathological even though direct comparison with tissue data cannot be made.

In most tissues the effects of Scarb1-deficiency on the FC/TC ratio were modest. The exceptions were ovary- and testes fat, (−50 and −35% respectively), ovaries (+70%) and especially adrenals in which the FC/TC ratio increased 400 and 2400% for females and males respectively, an effect due to profound reduction of CE, −85 and −95% for females and males respectively. Thus, of all the tissues the adrenals, the most CE-rich tissue studied, appear to be the most dependent on Scarb1 for CE delivery. A low adrenal-CE has been implicated in primary adrenal insufficiency in Scarb1$^{-/-}$ mice.[45]

Differences in tissue mol% FC could be due to differential FC efflux or FC conversion to CE; however, the latter mechanism does not explain the differences because CE do not transfer spontaneously, and mice do not express cholesteryl ester transfer protein. Moreover, the correlations between tissue mol% FC and CE were low ($r^2 = 0.11$; Supplementary Figure V A, B). Alternatively, tissue FC efflux, which occurs via both diffusion and

transporter mechanisms, could be different. Because diffusional efflux is a function of PL composition[76] on the donor surface, no difference in FC efflux is expected to occur by this mechanism. Tissues that maintain FC homeostasis may use transporters to export excess FC, but this was not uniformly observed. Although there were differences in the expression of ABCA1 and ABCG1 across the tissues studied, tissues that maintained good FC homeostasis were distributed over the entire range of transporter expression with that of lung being the second highest and heart being the second lowest (Supplementary Figure V C).[77] In addition, ABCA1 is an unlikely mediator of FC flux between erythrocytes and HDL.[78] First, FC efflux from erythrocytes to APOA1 was almost nil despite a high erythrocyte-ABCA1 content. Second, ABCA1 silencing or chemical inhibition did not inhibit FC efflux. Lastly, FC flux between erythrocytes and lipoproteins from $Abca1^{+/+}$ and $Abca1^{-/-}$ mice were similar. Although a bioinformatics analysis identified ABCA7, ABCG5, lipoprotein lipase, and mitochondrial translocator protein as candidate mediators of FC flux,[78] none have been tested. In addition, only ABCG5, a functional half-transporter, has an activity that directly relates to sterol transport, but only when associated with its co-transporter, ABCG8. Lastly, FC responsive tissues did not cluster according to Scarb1 expression; heart and lung, both of which had higher FC content in $Scarb1^{-/-}$ than WT mice, exhibited low and moderate Scarb1 expression (Supplementary Figure V D). Given the high Scarb1 expression in adrenals, it is not unexpected to see a profound reduction in adrenal CE content among $Scarb1^{-/-}$ mice.

Lastly, there could be differential tissue perfusion. Being in constant contact with plasma, one would expect erythrocytes, as observed, to show greater differences in FC accretion in $Scarb1^{-/-}$ than WT mice. Differential perfusion again seems unlikely to explain differences in FC accretion in tissues. Brain, which is well perfused, did not differ in the mol% FC in $Scarb1^{-/-}$ or WT mice. Brain contains 25 % of whole-body FC, but brain FC is derived from in situ synthesis. In humans there is little evidence for plasma-to-brain FC transfer,[72] a finding consistent with a blood-brain FC barrier. Thus, other factors that remain to be determined must control tissue-specific differences in FC accretion.

In vitro FC distribution between macrophages and HDL is governed by mass action such that FC-rich macrophages are a source of efflux to HDL,[79] and FC-rich HDL is a source of influx to cells, a correlation not previously tested in vivo. We asked whether differences in FC bioavailability, mostly as HDL-FC, differentially contributed to tissue FC content in WT and $Scarb1^{-/-}$ mice. Higher FC content, which was only observed in some tissues, could not be explained by differential CE formation, FC transporters, or perfusion. Candidate effectors cited by others also do not appear to be involved in differential FC accretion. According to the increase in mol% FC, sites that were most profoundly altered by Scarb1-deletion were ovaries (+80%), erythrocytes (+23%), heart (+21%), and macrophages (+300%); although adrenal-FC content was not greatly altered by Scarb1 deletion, the CE content was reduced by >85%. Among $Scarb1^{-/-}$ mice, these tissue sites are also respectively associated with female infertility,[47, 48] impaired cell maturation,[43, 44] cardiac dysfunction,[41] atherothrombosis,[30, 42, 80] and adrenal insufficiency.[45] Conversely, tissues from $Scarb1^{-/-}$ mice that had a mol% FC similar to those of WT mice exhibited no obvious pathologies suggesting that they have a FC defense system that remains to be identified. Unlike most previous studies, which combined the results of male and female mice, we analyzed male

and female mice separately and found that Scarb1 deletion increased the number of tissue sites with different lipid composition among male and female mice. Moreover, plasma FC clearance kinetics were also sex-dependent. The source of the sex-dependent differences could be estrogen-induced, either indirectly or directly. Among humans, plasma HDL-C concentrations are higher among females.[81] However, in contrast to the profound genotype-specific differences in HDL-C concentrations, sex-dependent differences in mouse HDL-C concentrations were small and not significant and those for mol% HDL-FC were nil. This suggests that the sex-dependent differences in plasma HDL-FC clearance kinetics and tissue-FC content are a direct effect of estrogen on these tissues by a mechanism that is currently not known.

There are some limiting considerations. Although genetically-altered mice and complementary biophysical studies can inform about the role of FC vs. CE in metabolism, mouse and human cholesterol metabolisms are different. Mice lack cholesteryl ester transfer protein, which in humans exchanges HDL- and LDL-CE for VLDL-TG.[82] The acyl-chain specificities of human and rodent LCAT are different.[83, 84] Tissues are multicellular so the tissue-lipid composition reflects that of the dominant cell type without informing about other minor cell types that may be more relevant to whole body cholesterol metabolism and its regulation. In some other studies, human SCARB1-deficiency[68] and three common SCARB1 non-coding variants that associate with higher HDL-C concentrations[85] conferred increased ASCVD risk. A subsequent study affirmed this finding[86] and demonstrated ASCVD heritability as a consequence of a human SCARB1 variant. The role of FC bioavailability in these ASCVD pathologies is unknown.

FC and CE have metabolic itineraries that likely impart different health risks. Nevertheless, most clinical trials of lipid-lowering therapies correlate ASCVD events with HDL- and LDL-total cholesterol rather than to FC and CE. Thus, the relationship between plasma and/or HDL-FC, which is important, is not adequately understood. Our observations provide a rationale for testing new therapeutics for dysfunctional HDL with underlying HDL-FC hyper-bioavailability and for identifying differences in HDL-FC to macrophage influx among patients with very high plasma HDL concentrations and ASCVD.

Supplementary Material

Refer to Web version on PubMed Central for supplementary material.

Acknowledgements:

Abbreviations:

HDL	high density lipoproteins
LDL	low density lipoproteins

Scarb1	scavenger receptor class B member 1
WT	wild-type
ASCVD	atherosclerotic cardiovascular disease
FC	free cholesterol

References

1. Classics in arteriosclerosis research: On experimental cholesterin steatosis and its significance in the origin of some pathological processes by N. Anitschkow and S. Chalatow, translated by Mary Z. Pelias, 1913. Arteriosclerosis. 1983;3:178–82. [PubMed: 6340651]

2. Gofman JW, Young W and Tandy R. Ischemic heart disease, atherosclerosis, and longevity. Circulation. 1966;34:679–97. [PubMed: 5921763]

3. Gordon T, Castelli WP, Hjortland MC, Kannel WB and Dawber TR. High density lipoprotein as a protective factor against coronary heart disease. The Framingham Study. Am J Med. 1977;62:707–14. [PubMed: 193398]

4. Schwartz GG, Olsson AG, Abt M, Ballantyne CM, Barter PJ, Brumm J, Chaitman BR, Holme IM, Kallend D, Leiter LA, Leitersdorf E, McMurray JJ, Mundl H, Nicholls SJ, Shah PK, Tardif JC, Wright RS and dal OI. Effects of dalcetrapib in patients with a recent acute coronary syndrome. N Engl J Med. 2012;367:2089–99. [PubMed: 23126252]

5. Tall AR, Yvan-Charvet L and Wang N. The failure of torcetrapib: was it the molecule or the mechanism? Arterioscler Thromb Vasc Biol. 2007;27:257–60. [PubMed: 17229967]

6. Zhao HP and Xiang BR. Discontinued cardiovascular drugs in 2013 and 2014. Expert Opin Investig Drugs. 2015;24:1083–92.

7. Boden WE, Probstfield JL, Anderson T, Chaitman BR, Desvignes-Nickens P, Koprowicz K, McBride R, Teo K and Weintraub W. Niacin in patients with low HDL cholesterol levels receiving intensive statin therapy. N Engl J Med. 2011;365:2255–67. [PubMed: 22085343]

8. Ko DT, Alter DA, Guo H, Koh M, Lau G, Austin PC, Booth GL, Hogg W, Jackevicius CA, Lee DS, Wijeysundera HC, Wilkins JT and Tu JV. High-Density Lipoprotein Cholesterol and Cause-Specific Mortality in Individuals Without Previous Cardiovascular Conditions: The CANHEART Study. J Am Coll Cardiol. 2016;68:2073–2083. [PubMed: 27810046]

9. Bowe B, Xie Y, Xian H, Balasubramanian S, Zayed MA and Al-Aly Z. High Density Lipoprotein Cholesterol and the Risk of All-Cause Mortality among U.S. Veterans. Clin J Am Soc Nephrol. 2016;11:1784–1793. [PubMed: 27515591]

10. Madsen CM, Varbo A and Nordestgaard BG. Extreme high high-density lipoprotein cholesterol is paradoxically associated with high mortality in men and women: two prospective cohort studies. Eur Heart J. 2017;38:2478–2486. [PubMed: 28419274]

11. Madsen CM and Nordestgaard BG. Is It Time for New Thinking About High-Density Lipoprotein? Arterioscler Thromb Vasc Biol. 2018;38:484–486. [PubMed: 29467220]

12. Hamer M, O'Donovan G and Stamatakis E. High-Density Lipoprotein Cholesterol and Mortality: Too Much of a Good Thing? Arterioscler Thromb Vasc Biol. 2018;38:669–672. [PubMed: 29326314]

13. Khera AV, Cuchel M, de la Llera-Moya M, Rodrigues A, Burke MF, Jafri K, French BC, Phillips JA, Mucksavage ML, Wilensky RL, Mohler ER, Rothblat GH and Rader DJ. Cholesterol efflux capacity, high-density lipoprotein function, and atherosclerosis. N Engl J Med. 2011;364:127–35. [PubMed: 21226578]

14. Toth PP, Barter PJ, Rosenson RS, Boden WE, Chapman MJ, Cuchel M, D'Agostino RB, Sr., Davidson MH, Davidson WS, Heinecke JW, Karas RH, Kontush A, Krauss RM, Miller M and Rader DJ. High-density lipoproteins: a consensus statement from the National Lipid Association. Journal of clinical lipidology. 2013;7:484–525. [PubMed: 24079290]

15. Rosenson RS, Brewer HB Jr., Davidson WS, Fayad ZA, Fuster V, Goldstein J, Hellerstein M, Jiang XC, Phillips MC, Rader DJ, Remaley AT, Rothblat GH, Tall ARand Yvan-Charvet L. Cholesterol

efflux and atheroprotection: advancing the concept of reverse cholesterol transport. Circulation. 2012;125:1905–19. [PubMed: 22508840]

16. Rosenson RS, Brewer HB Jr., Ansell BJ, Barter P, Chapman MJ, Heinecke JW, Kontush A, Tall ARand Webb NR. Dysfunctional HDL and atherosclerotic cardiovascular disease. Nature reviews Cardiology. 2015.

17. Rohatgi A, Khera A, Berry JD, Givens EG, Ayers CR, Wedin KE, Neeland IJ, Yuhanna IS, Rader DR, de Lemos JA and Shaul PW. HDL cholesterol efflux capacity and incident cardiovascular events. N Engl J Med. 2014;371:2383–93. [PubMed: 25404125]

18. Guerin M, Silvain J, Gall J, Darabi M, Berthet M, Frisdal E, Hauguel-Moreau M, Zeitouni M, Kerneis M, Lattuca B, Brugier D, Collet JP, Lesnik P and Montalescot G. Association of Serum Cholesterol Efflux Capacity With Mortality in Patients With ST-Segment Elevation Myocardial Infarction. J Am Coll Cardiol. 2018;72:3259–3269. [PubMed: 30573028]

19. Soria-Florido MT, Castaner O, Lassale C, Estruch R, Salas-Salvado J, Martinez-Gonzalez MA, Corella D, Ros E, Aros F, Elosua R, Lapetra J, Fiol M, Alonso-Gomez A, Gomez-Gracia E, Serra-Majem L, Pinto X, Bullo M, Ruiz-Canela M, Sorli JV, Hernaez A and Fito M. Dysfunctional High-Density Lipoproteins Are Associated With a Greater Incidence of Acute Coronary Syndrome in a Population at High Cardiovascular Risk: A Nested Case-Control Study. Circulation. 2020;141:444–453. [PubMed: 31941372]

20. Mutharasan RK, Thaxton CS, Berry J, Daviglus ML, Yuan C, Sun J, Ayers C, Lloyd-Jones DM and Wilkins JT. HDL efflux capacity, HDL particle size, and high-risk carotid atherosclerosis in a cohort of asymptomatic older adults: the Chicago Healthy Aging Study. J Lipid Res. 2017;58:600–606. [PubMed: 28049656]

21. Li XM, Tang WH, Mosior MK, Huang Y, Wu Y, Matter W, Gao V, Schmitt D, Didonato JA, Fisher EA, Smith JD and Hazen SL. Paradoxical association of enhanced cholesterol efflux with increased incident cardiovascular risks. Arterioscler Thromb Vasc Biol. 2013;33:1696–705. [PubMed: 23520163]

22. Josefs T, Wouters K, Tietge UJF, Annema W, Dullaart RPF, Vaisar T, Arts ICW, van der Kallen CJH, Stehouwer CDA, Schalkwijk CG, Goldberg IJ, Fisher EA and van Greevenbroek MMJ. High-density lipoprotein cholesterol efflux capacity is not associated with atherosclerosis and prevalence of cardiovascular outcome: The CODAM study. Journal of clinical lipidology. 2020;14:122–132 e4. [PubMed: 31791716]

23. de Vries R, Groen AK and Dullaart RP. Cholesterol efflux capacity and atherosclerosis. N Engl J Med. 2011;364:1473–4; author reply 1474–5.

24. Weibel GL, Drazul-Schrader D, Shivers DK, Wade AN, Rothblat GH, Reilly MP and de la Llera-Moya M. Importance of evaluating cell cholesterol influx with efflux in determining the impact of human serum on cholesterol metabolism and atherosclerosis. Arterioscler Thromb Vasc Biol. 2014;34:17–25. [PubMed: 24202308]

25. Johnson WJ, Bamberger MJ, Latta RA, Rapp PE, Phillips MC and Rothblat GH. The bidirectional flux of cholesterol between cells and lipoproteins. Effects of phospholipid depletion of high density lipoprotein. J Biol Chem. 1986;261:5766–76. [PubMed: 3700371]

26. Johnson WJ, Mahlberg FH, Chacko GK, Phillips MC and Rothblat GH. The influence of cellular and lipoprotein cholesterol contents on the flux of cholesterol between fibroblasts and high density lipoprotein. J Biol Chem. 1988;263:14099–106. [PubMed: 2844757]

27. Phillips MC, Johnson WJ and Rothblat GH. Mechanisms and consequences of cellular cholesterol exchange and transfer. Biochim Biophys Acta. 1987;906:223–76. [PubMed: 3297153]

28. Pownall HJ, Rosales C, Gillard BK and Gotto AM, Jr. High-density lipoproteins, reverse cholesterol transport and atherogenesis. Nature reviews Cardiology. 2021.

29. Lund-Katz S, Hammerschlag B and Phillips MC. Kinetics and mechanism of free cholesterol exchange between human serum high- and low-density lipoproteins. Biochemistry. 1982;21:2964–9. [PubMed: 7104306]

30. Van Eck M, Twisk J, Hoekstra M, Van Rij BT, Van der Lans CA, Bos IS, Kruijt JK, Kuipers F and Van Berkel TJ. Differential effects of scavenger receptor BI deficiency on lipid metabolism in cells of the arterial wall and in the liver. J Biol Chem. 2003;278:23699–705. [PubMed: 12639961]

31. Ma K, Forte T, Otvos JD and Chan L. Differential additive effects of endothelial lipase and scavenger receptor-class B type I on high-density lipoprotein metabolism in knockout mouse models. Arterioscler Thromb Vasc Biol. 2005;25:149–54. [PubMed: 15539616]

32. Picardo M, Massey JB, Kuhn DE, Gotto AM Jr., Gianturco SHand Pownall HJ. Partially reassembled high density lipoproteins. Effects on cholesterol flux, synthesis, and esterification in normal human skin fibroblasts. Arteriosclerosis. 1986;6:434–41. [PubMed: 3729799]

33. Johnson WJ, Mahlberg FH, Rothblat GH and Phillips MC. Cholesterol transport between cells and high-density lipoproteins. Biochim Biophys Acta. 1991;1085:273–98. [PubMed: 1911862]

34. Yancey PG, de la Llera-Moya M, Swarnakar S, Monzo P, Klein SM, Connelly MA, Johnson WJ, Williams DL and Rothblat GH. High density lipoprotein phospholipid composition is a major determinant of the bi-directional flux and net movement of cellular free cholesterol mediated by scavenger receptor BI. J Biol Chem. 2000;275:36596–604. [PubMed: 10964930]

35. Ji Y, Wang N, Ramakrishnan R, Sehayek E, Huszar D, Breslow JL and Tall AR. Hepatic scavenger receptor BI promotes rapid clearance of high density lipoprotein free cholesterol and its transport into bile. J Biol Chem. 1999;274:33398–402. [PubMed: 10559220]

36. Xu B, Gillard BK, Gotto AM Jr., Rosales C and Pownall HJ. ABCA1-Derived Nascent High-Density Lipoprotein-Apolipoprotein AI and Lipids Metabolically Segregate. Arterioscler Thromb Vasc Biol. 2017;37:2260–2270. [PubMed: 29074589]

37. Schwartz CC, VandenBroek JM and Cooper PS. Lipoprotein cholesteryl ester production, transfer, and output in vivo in humans. J Lipid Res. 2004;45:1594–607. [PubMed: 15145983]

38. Thuahnai ST, Lund-Katz S, Williams DL and Phillips MC. Scavenger receptor class B, type I-mediated uptake of various lipids into cells. Influence of the nature of the donor particle interaction with the receptor. J Biol Chem. 2001;276:43801–8. [PubMed: 11564739]

39. Zhang S, Picard MH, Vasile E, Zhu Y, Raffai RL, Weisgraber KH and Krieger M. Diet-induced occlusive coronary atherosclerosis, myocardial infarction, cardiac dysfunction, and premature death in scavenger receptor class B type I-deficient, hypomorphic apolipoprotein ER61 mice. Circulation. 2005;111:3457–64. [PubMed: 15967843]

40. Rigotti A, Trigatti BL, Penman M, Rayburn H, Herz J and Krieger M. A targeted mutation in the murine gene encoding the high density lipoprotein (HDL) receptor scavenger receptor class B type I reveals its key role in HDL metabolism. Proc Natl Acad Sci U S A. 1997;94:12610–5. [PubMed: 9356497]

41. Braun A, Trigatti BL, Post MJ, Sato K, Simons M, Edelberg JM, Rosenberg RD, Schrenzel M and Krieger M. Loss of SR-BI expression leads to the early onset of occlusive atherosclerotic coronary artery disease, spontaneous myocardial infarctions, severe cardiac dysfunction, and premature death in apolipoprotein E-deficient mice. Circ Res. 2002;90:270–6. [PubMed: 11861414]

42. Braun A, Zhang S, Miettinen HE, Ebrahim S, Holm TM, Vasile E, Post MJ, Yoerger DM, Picard MH, Krieger JL, Andrews NC, Simons M and Krieger M. Probucol prevents early coronary heart disease and death in the high-density lipoprotein receptor SR-BI/apolipoprotein E double knockout mouse. Proc Natl Acad Sci U S A. 2003;100:7283–8. [PubMed: 12771386]

43. Meurs I, Hoekstra M, van Wanrooij EJ, Hildebrand RB, Kuiper J, Kuipers F, Hardeman MR, Van Berkel TJ and Van Eck M. HDL cholesterol levels are an important factor for determining the lifespan of erythrocytes. Exp Hematol. 2005;33:1309–19. [PubMed: 16263415]

44. Holm TM, Braun A, Trigatti BL, Brugnara C, Sakamoto M, Krieger M and Andrews NC. Failure of red blood cell maturation in mice with defects in the high-density lipoprotein receptor SR-BI. Blood. 2002;99:1817–24. [PubMed: 11861300]

45. Hoekstra MIdentification of scavenger receptor BI as a potential screening candidate for congenital primary adrenal insufficiency in humans. Am J Physiol Endocrinol Metab. 2020;319:E102–E104. [PubMed: 32369415]

46. Guo L, Zheng Z, Ai J, Howatt DA, Mittelstadt PR, Thacker S, Daugherty A, Ashwell JD, Remaley AT and Li XA. Scavenger receptor BI and high-density lipoprotein regulate thymocyte apoptosis in sepsis. Arterioscler Thromb Vasc Biol. 2014;34:966–75. [PubMed: 24603680]

47. Miettinen HE, Rayburn H and Krieger M. Abnormal lipoprotein metabolism and reversible female infertility in HDL receptor (SR-BI)-deficient mice. J Clin Invest. 2001;108:1717–22. [PubMed: 11733567]

48. Yesilaltay A, Dokshin GA, Busso D, Wang L, Galiani D, Chavarria T, Vasile E, Quilaqueo L, Orellana JA, Walzer D, Shalgi R, Dekel N, Albertini DF, Rigotti A, Page DC and Krieger M. Excess cholesterol induces mouse egg activation and may cause female infertility. Proc Natl Acad Sci U S A. 2014;111:E4972–80. [PubMed: 25368174]

49. Yesilaltay A, Morales MG, Amigo L, Zanlungo S, Rigotti A, Karackattu SL, Donahee MH, Kozarsky KF and Krieger M. Effects of hepatic expression of the high-density lipoprotein receptor SR-BI on lipoprotein metabolism and female fertility. Endocrinology. 2006;147:1577–88. [PubMed: 16410302]

50. Havel RJ, Eder HA and Bragdon JH. The distribution and chemical composition of ultracentrifugally separated lipoproteins in human serum. J Clin Invest. 1955;34:1345–53. [PubMed: 13252080]

51. Schumaker VN and Puppione DL. Sequential flotation ultracentrifugation. Methods Enzymol. 1986;128:155–70. [PubMed: 3724500]

52. Gillard BK, Rosales C, Pillai BK, Lin HY, Courtney HS and Pownall HJ. Streptococcal serum opacity factor increases the rate of hepatocyte uptake of human plasma high-density lipoprotein cholesterol. Biochemistry. 2010;49:9866–73. [PubMed: 20879789]

53. Davidson WS, Heink A, Sexmith H, Melchior JT, Gordon SM, Kuklenyik Z, Woollett L, Barr JR, Jones JI, Toth CA and Shah AS. The effects of apolipoprotein B depletion on HDL subspecies composition and function. J Lipid Res. 2016;57:674–86. [PubMed: 26908829]

54. de la Llera-Moya M, Drazul-Schrader D, Asztalos BF, Cuchel M, Rader DJ and Rothblat GH. The ability to promote efflux via ABCA1 determines the capacity of serum specimens with similar high-density lipoprotein cholesterol to remove cholesterol from macrophages. Arterioscler Thromb Vasc Biol. 2010;30:796–801. [PubMed: 20075420]

55. Tchoua U, Gillard BK and Pownall HJ. HDL superphospholipidation enhances key steps in reverse cholesterol transport. Atherosclerosis. 2010;209:430–5. [PubMed: 19892352]

56. Acton S, Rigotti A, Landschulz KT, Xu S, Hobbs HH and Krieger M. Identification of scavenger receptor SR-BI as a high density lipoprotein receptor. Science. 1996;271:518–20. [PubMed: 8560269]

57. Rosales C, Tang D, Gillard BK, Courtney HS and Pownall HJ. Apolipoprotein E mediates enhanced plasma high-density lipoprotein cholesterol clearance by low-dose streptococcal serum opacity factor via hepatic low-density lipoprotein receptors in vivo. Arterioscler Thromb Vasc Biol. 2011;31:1834–41. [PubMed: 21597008]

58. Gillard BK, Rodriguez PJ, Fields DW, Raya JL, Lagor WR, Rosales C, Courtney HS, Gotto AM Jr. and Pownall HJ. Streptococcal serum opacity factor promotes cholesterol ester metabolism and bile acid secretion in vitro and in vivo. Biochim Biophys Acta. 2016;1861:196–204. [PubMed: 26709142]

59. Radin NS. Extraction of tissue lipids with a solvent of low toxicity. Methods Enzymol. 1981;72:5–7. [PubMed: 7311848]

60. Pownall HJ, Bick DL and Massey JB. Spontaneous phospholipid transfer: development of a quantitative model. Biochemistry. 1991;30:5696–700. [PubMed: 2043612]

61. Temel RE, Trigatti B, DeMattos RB, Azhar S, Krieger M and Williams DL. Scavenger receptor class B, type I (SR-BI) is the major route for the delivery of high density lipoprotein cholesterol to the steroidogenic pathway in cultured mouse adrenocortical cells. Proc Natl Acad Sci U S A. 1997;94:13600–5. [PubMed: 9391072]

62. Hatzopoulos AK, Rigotti A, Rosenberg RD and Krieger M. Temporal and spatial pattern of expression of the HDL receptor SR-BI during murine embryogenesis. J Lipid Res. 1998;39:495–508. [PubMed: 9548583]

63. Landschulz KT, Pathak RK, Rigotti A, Krieger M and Hobbs HH. Regulation of scavenger receptor, class B, type I, a high density lipoprotein receptor, in liver and steroidogenic tissues of the rat. J Clin Invest. 1996;98:984–95. [PubMed: 8770871]

64. Thomson WOn the equilibrium of vapour at a curved surface of liquid. Philosophical Magazine1871;42:5.

65. Huszar D, Varban ML, Rinninger F, Feeley R, Arai T, Fairchild-Huntress V, Donovan MJ and Tall AR. Increased LDL cholesterol and atherosclerosis in LDL receptor-deficient mice with attenuated

expression of scavenger receptor B1. Arterioscler Thromb Vasc Biol. 2000;20:1068–73. [PubMed: 10764675]

66. Cedo L, Metso J, Santos D, Garcia-Leon A, Plana N, Sabate-Soler S, Rotllan N, Rivas-Urbina A, Mendez-Lara KA, Tondo M, Girona J, Julve J, Pallares V, Benitez-Amado A, Llorente Cortes V, Perez A, Gomez-Coronado D, Ruotsalainen AK, Levonen AL, Sanchez-Quesada JL, Masana L, Kovanen PT, Jauhiainen MS, Lee-Rueckert M, Blanco-Vaca F and Escola-Gil JC. LDL Receptor Regulates the Reverse Transport of Macrophage-Derived Unesterified Cholesterol via Concerted Action of the HDL-LDL Axis: Insight from Mouse Models. Circ Res. 2020.

67. de Boer JF, Schonewille M, Dikkers A, Koehorst M, Havinga R, Kuipers F, Tietge UJ and Groen AK. Transintestinal and Biliary Cholesterol Secretion Both Contribute to Macrophage Reverse Cholesterol Transport in Rats-Brief Report. Arterioscler Thromb Vasc Biol. 2017;37:643–646. [PubMed: 28232326]

68. Zanoni P, Khetarpal SA, Larach DB, Hancock-Cerutti WF, Millar JS, Cuchel M, DerOhannessian S, Kontush A, Surendran P, Saleheen D, Trompet S, Jukema JW, De Craen A, Deloukas P, Sattar N, Ford I, Packard C, Majumder A, Alam DS, Di Angelantonio E, Abecasis G, Chowdhury R, Erdmann J, Nordestgaard BG, Nielsen SF, Tybjaerg-Hansen A, Schmidt RF, Kuulasmaa K, Liu DJ, Perola M, Blankenberg S, Salomaa V, Mannisto S, Amouyel P, Arveiler D, Ferrieres J, Muller-Nurasyid M, Ferrario M, Kee F, Willer CJ, Samani N, Schunkert H, Butterworth AS, Howson JM, Peloso GM, Stitziel NO, Danesh J, Kathiresan S, Rader DJ, Consortium CHDE, Consortium CAE and Global Lipids Genetics C. Rare variant in scavenger receptor BI raises HDL cholesterol and increases risk of coronary heart disease. Science. 2016;351:1166–71. [PubMed: 26965621]

69. Vasudevan M, Tchoua U, Gillard BK, Jones PH, Ballantyne CM and Pownall HJ. Modest diet-induced weight loss reduces macrophage cholesterol efflux to plasma of patients with metabolic syndrome. Journal of clinical lipidology. 2013;7:661–70. [PubMed: 24314365]

70. Schwartz CC, Vlahcevic ZR, Berman M, Meadows JG, Nisman RM and Swell L. Central role of high density lipoprotein in plasma free cholesterol metabolism. J Clin Invest. 1982;70:105–16. [PubMed: 6953075]

71. Thacker SG, Rousset X, Esmail S, Zarzour A, Jin X, Collins HL, Sampson M, Stonik J, Demosky S, Malide DA, Freeman L, Vaisman BL, Kruth HS, Adelman SJ and Remaley AT. Increased plasma cholesterol esterification by LCAT reduces diet-induced atherosclerosis in SR-BI knockout mice. J Lipid Res. 2015;56:1282–95. [PubMed: 25964513]

72. Dietschy JM and Turley SD. Cholesterol metabolism in the brain. Curr Opin Lipidol. 2001;12:105–12. [PubMed: 11264981]

73. Rodriguez PJ, Gillard BK, Barosh R, Gotto AM Jr., Rosales C and Pownall HJ. Neo High-Density Lipoprotein Produced by the Streptococcal Serum Opacity Factor Activity against Human High-Density Lipoproteins Is Hepatically Removed via Dual Mechanisms. Biochemistry. 2016;55:5845–5853. [PubMed: 27662183]

74. Gillard BK, Bassett GR, Gotto AM Jr., Rosales C and Pownall HJ. Scavenger receptor B1 (SR-B1) profoundly excludes high density lipoprotein (HDL) apolipoprotein AII as it nibbles HDL-cholesteryl ester. J Biol Chem. 2017;292:8864–8873. [PubMed: 28373285]

75. Quan G, Xie C, Dietschy JM and Turley SD. Ontogenesis and regulation of cholesterol metabolism in the central nervous system of the mouse. Brain Res Dev Brain Res. 2003;146:87–98. [PubMed: 14643015]

76. Lund-Katz S, Laboda HM, McLean LR and Phillips MC. Influence of molecular packing and phospholipid type on rates of cholesterol exchange. Biochemistry. 1988;27:3416–23. [PubMed: 3390441]

77. Fagerberg L, Hallstrom BM, Oksvold P, Kampf C, Djureinovic D, Odeberg J, Habuka M, Tahmasebpoor S, Danielsson A, Edlund K, Asplund A, Sjostedt E, Lundberg E, Szigyarto CA, Skogs M, Takanen JO, Berling H, Tegel H, Mulder J, Nilsson P, Schwenk JM, Lindskog C, Danielsson F, Mardinoglu A, Sivertsson A, von Feilitzen K, Forsberg M, Zwahlen M, Olsson I, Navani S, Huss M, Nielsen J, Ponten F and Uhlen M. Analysis of the human tissue-specific expression by genome-wide integration of transcriptomics and antibody-based proteomics. Molecular & cellular proteomics : MCP. 2014;13:397–406.

78. Ohkawa R, Low H, Mukhamedova N, Fu Y, Lai SJ, Sasaoka M, Hara A, Yamazaki A, Kameda T, Horiuchi Y, Meikle PJ, Pernes G, Lancaster GI, Ditiatkovski M, Nestel P, Vaisman BL, Sviridov D, Murphy AJ, Remaley AT, Sviridov D and Tozuka M. Cholesterol transport between red blood cells and lipoproteins contributes to cholesterol metabolism in blood. J Lipid Res. 2020.

79. Sankaranarayanan S, de la Llera-Moya M, Drazul-Schrader D, Asztalos BF, Weibel GL and Rothblat GH. Importance of macrophage cholesterol content on the flux of cholesterol mass. J Lipid Res. 2010;51:3243–9. [PubMed: 20713652]

80. Korporaal SJ, Meurs I, Hauer AD, Hildebrand RB, Hoekstra M, Cate HT, Pratico D, Akkerman JW, Van Berkel TJ, Kuiper J and Van Eck M. Deletion of the high-density lipoprotein receptor scavenger receptor BI in mice modulates thrombosis susceptibility and indirectly affects platelet function by elevation of plasma free cholesterol. Arterioscler Thromb Vasc Biol. 2011;31:34–42. [PubMed: 21051668]

81. Schaefer EJ. Clinical, biochemical, and genetic features in familial disorders of high density lipoprotein deficiency. Arteriosclerosis. 1984;4:303–22. [PubMed: 6431953]

82. Pownall HJ, Brauchi D, Kilinc C, Osmundsen K, Pao Q, Payton-Ross C, Gotto AM Jr. and Ballantyne CM. Correlation of serum triglyceride and its reduction by omega-3 fatty acids with lipid transfer activity and the neutral lipid compositions of high-density and low-density lipoproteins. Atherosclerosis. 1999;143:285–97. [PubMed: 10217357]

83. Pownall HJ, Pao Q and Massey JB. Isolation and specificity of rat lecithin: cholesterol acyltransferase: comparison with the human enzyme using reassembled high-density lipoproteins containing ether analogs of phosphatidylcholine. Biochim Biophys Acta. 1985;833:456–62. [PubMed: 3918579]

84. Pownall HJ, Pao Q and Massey JB. Acyl chain and headgroup specificity of human plasma lecithin:cholesterol acyltransferase. Separation of matrix and molecular specificities. J Biol Chem. 1985;260:2146–52. [PubMed: 3918998]

85. Helgadottir A, Sulem P, Thorgeirsson G, Gretarsdottir S, Thorleifsson G, Jensson BO, Arnadottir GA, Olafsson I, Eyjolfsson GI, Sigurdardottir O, Thorsteinsdottir U, Gudbjartsson DF, Holm H and Stefansson K. Rare SCARB1 mutations associate with high-density lipoprotein cholesterol but not with coronary artery disease. Eur Heart J. 2018;39:2172–2178. [PubMed: 29596577]

86. Koenig SN, Sucharski HC, Jose E, Dudley EK, Madiai F, Cavus O, Argall AD, Williams J, Murphy NP, Keith CB, El Refaey M, Gumina R, Boudoulas KD, Milks MW, Sofowora G, Smith SA, Hund TJ, Wright NT, Bradley E, Zareba KM, Wold LE, Mazzaferri EL Jr. and Mohler PJ. Inherited Variants in SCARB1 Cause Severe Early-Onset Coronary Artery Disease. Circ Res. 2021.

Highlights

Given that phospholipid (PL) is the FC solvent, HDL-mol% FC = $100\% \times mol_{FC}/(mol_{FC} + mol_{PL})$ is a metric for plasma HDL-FC bioavailability, which is increased by Scarb1-deficiency.

The rate of HDL-FC clearance is only modestly reduced by Scarb1-deficiency ($\sim -30\%$) so that most HDL-FC clearance likely occurs via spontaneous transfer or other lipoprotein receptors.

Independent of genotype, plasma HDL-FC clearance and tissue-accretion are sex-dependent.

The mass of Scarb1$^{-/-}$ mouse-HDL FC influx into J774 macrophages was greater than that from WT whereas the rates of the reverse process, efflux, were similar.

Increased tissue mol% FC produced by Scarb1-deficiency is associated with pathologies in those tissues whereas tissues with preserved FC homeostasis exhibited no overt pathologies.

Given that FC efflux predicts atherosclerosis, our findings provide a rationale for comparing FC influx from HDL of patients with and without ASCVD to macrophages to determine whether HDL-FC influx is atherogenic.
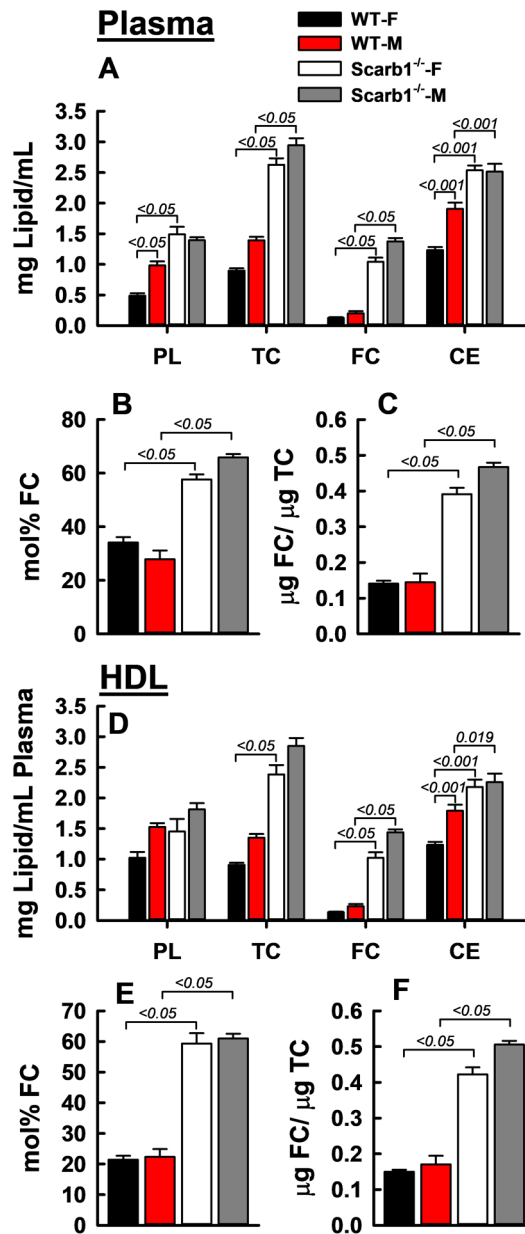
Figure 1:

Plasma (A–C) and HDL (D–F) Lipid Concentrations of Male (M) and Female (F) WT and Scarb1$^{-/-}$ Mice. HDL were obtained from individual mouse plasma by heparin-manganese depletion of APOB lipoproteins. Bars are mean ± SEM. Numbers of mice per group are: WT-F (n = 12), WT-M (n = 10), Scarb1$^{-/-}$-F (n = 11) and Scarb1$^{-/-}$-M (n = 5). ANOVA and pairwise comparisons were calculated as described in Methods. P-values for significantly different pairwise comparisons (p <0.05) are indicated over brackets.
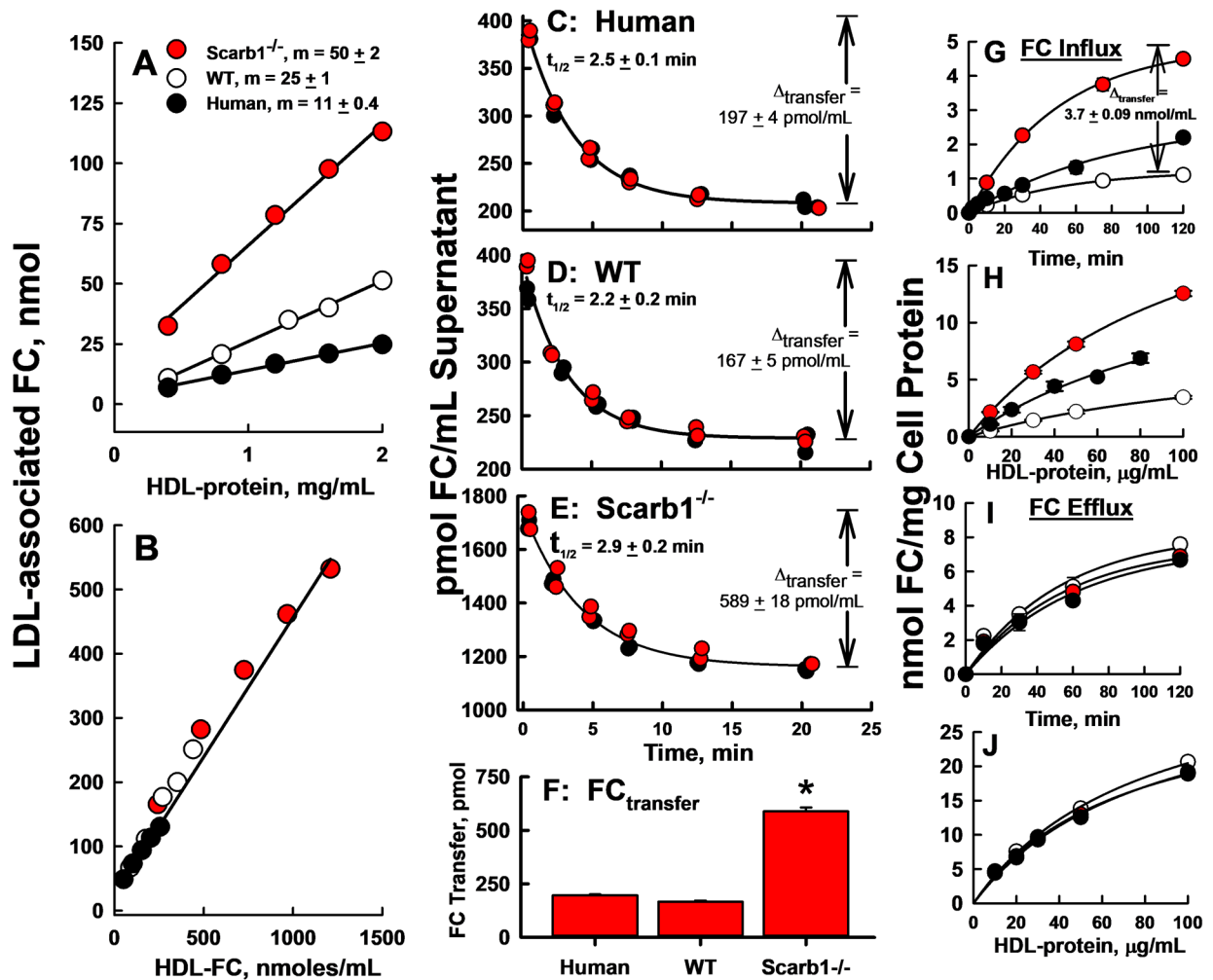
Figure 2:

HDL-FC Transfer to human LDL and J774 Macrophages. **A, B**: Equilibrium distribution of [³H]FC between various HDL and human LDL according to HDL-protein (**A**) and HDL-FC (**B**). The specific activities of WT mouse, Scarb1⁻/⁻ mouse and human HDL-FC were 21,488, 7,942, and 38,233 dpm/nmol FC respectively. In **A**, m, the slopes of the linear regression lines, are different, p 0.0001 for all three curves. In **B**, where transfer is plotted vs. starting HDL-FC, data for the three HDL fall on a single line. **C–E:** Kinetics of HDL-[³H]FC Transfer to human LDL as labeled. The red and black symbols are from two independent experiments, and the lines are exponential decay fits of the combined data, as described in Methods. **F**: Extent of FC transfer from HDL to LDL at the asymptote, i.e., kinetic equilibrium, calculated from **C–E**. FC transferred from Scarb1⁻/⁻ HDL > WT HDL (p < 0.0001). **G–J**: FC Flux between HDL and J774 Macrophages. **G, H**: FC influx from HDL to macrophages according to time (**G**) at 20 μg HDL-protein/mL and dose at 2 h (**H**). [³H]FC specific radioactivities were 40,767, 9,242 and 15,247 dpm/nmol FC respectively for human, WT, and Scarb1⁻/⁻ HDL. At all times and doses, FC influx from SCARB1⁻/⁻ HDL > WT HDL (p<0.0001). **I, J**: FC efflux from macrophages to HDL, time course (**I**; 20 μg HDL-protein/mL) and dose response (2 h; **J**). The plots are representative of two to three

independent experiments, each done in triplicate. The points are mean ± SD with error bars sometimes smaller than the symbols.
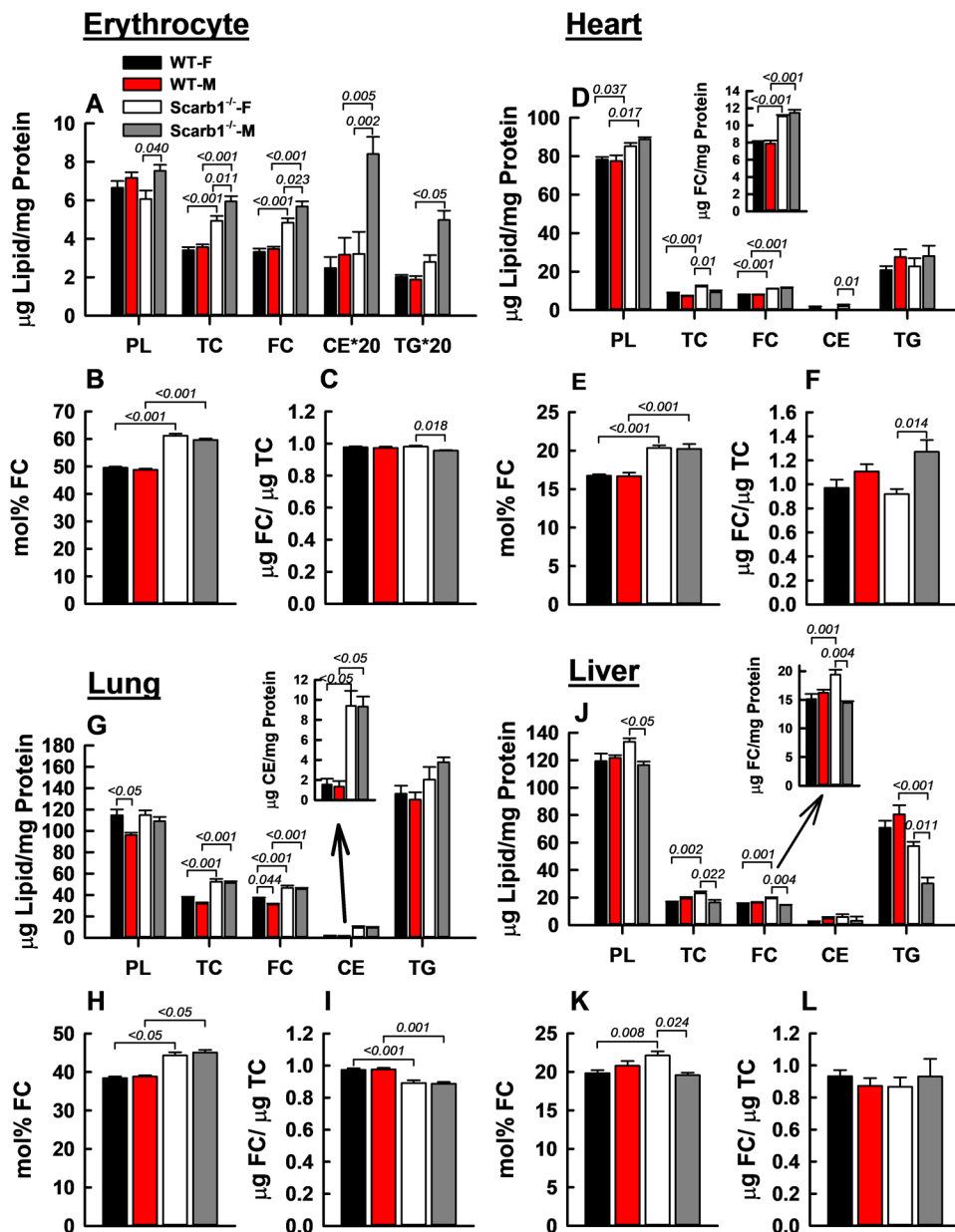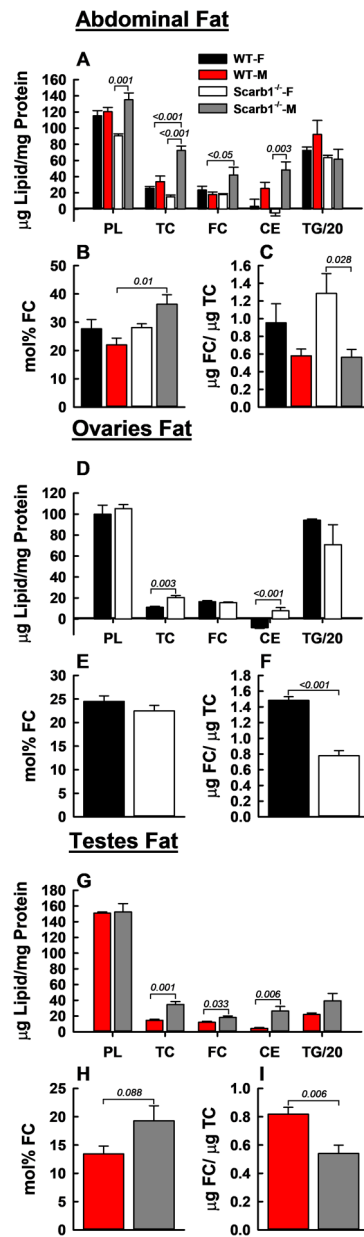
Figure 3:

FC Accretion and Lipid Composition of Erythrocytes, Heart, Lung, and Liver. Within each group—A–C (erythrocytes), D–F (heart), G–I (lung), and J–L (liver)—the respective panels provide the lipid composition relative to protein (W/W), mol% FC, and the FC/total cholesterol (TC) ratio (W/W). Bars are mean ± SEM. Statistics are as described in Figure 1 legend. Mice/group are as follows: Erythrocytes, WT-F (n = 6), WT-M (n = 4), Scarb1$^{-/-}$-F (n = 6) and Scarb1$^{-/-}$-M (n = 8); for heart, lung and liver WT-F (n = 12), WT-M (n = 10), Scarb1$^{-/-}$-F (n = 11) and Scarb1$^{-/-}$-M (n = 5).

Figure 4:
FC Accretion and Lipid Compositions in Abdominal-, Ovary-, and Testes-Fat. TG values are at 1/20 scale vs. other lipids. Within each group—A–C (abdominal fat), E–F (ovary fat), and G–I (testes fat)—the respective panels provide lipid composition vs. protein (W/W), mol% FC, and FC/TC ratio (W/W). Bars are mean ± SEM. Mice/group are as follows: Abdominal fat, WT-F (n = 4), WT-M (n = 5), Scarb1$^{-/-}$-F (n = 4) and Scarb1$^{-/-}$-M (n = 5); ovary fat, WT-F (n = 5) and Scarb1$^{-/-}$-F (n = 4); testis fat, WT-M (n = 5), and Scarb1$^{-/-}$-M (n = 5). Statistics are as described in Figure 1 legend. In Panels A and D, some values for CE that were at the detection limit are nevertheless shown with their SEM for completeness.
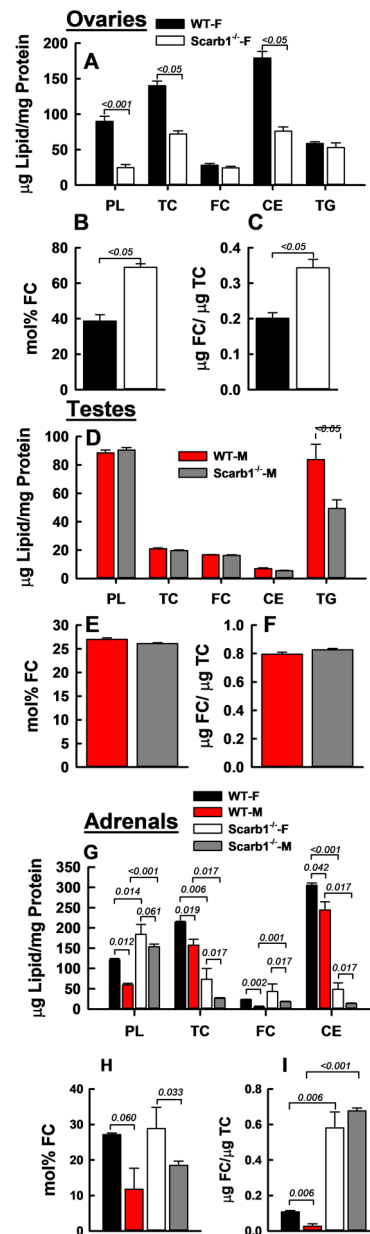
Figure 5:
FC Accretion and Lipid Compositions in Ovaries (A–C), Testes (D–F), and Adrenals (G–I). Bars are mean ± SEM. Numbers of mice per group for ovaries were as follows: WT-F (n = 12), Scarb1$^{-/-}$-F (n = 10). For testis: WT-M (n = 10), Scarb1$^{-/-}$-M (n = 5). For adrenals: WT-F (n = 3); WT-M (n = 3); Scarb1$^{-/-}$-F (n = 3); Scarb1$^{-/-}$ M (n = 7). Statistics as described in Figure 1 legend.
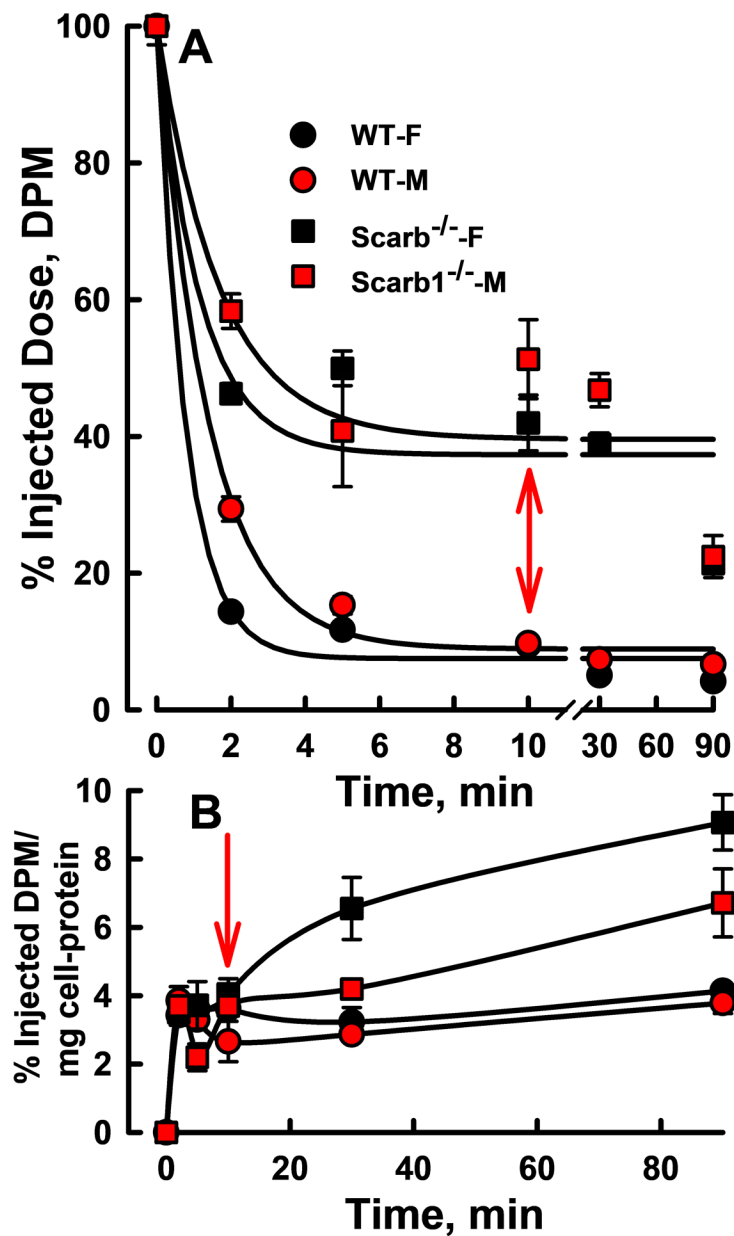
Figure 6:

In vivo HDL-FC Kinetics. A) Plasma decay kinetics of autologous HDL-[^{3}H]FC in female and male WT and Scarb1$^{-/-}$ mice. B) In the same experiments, erythrocyte-[^{3}H]FC. Mice of each genotype/sex (n = 3–4) were injected and blood collected at each time point; symbols are mean ± SD. The respective specific activities of the injected WT and Scarb1$^{-/-}$ mouse HDL (50 μg protein/mouse) were 6,160 and 5,110 dpm/μg. Injected HDL-FC < 1% of endogenous FC. Rate constants and statistical comparisons are given in Supplementary Table IV.